DYNAMIC AND STATIC CHARACTERIZATION OF THE PLANIMETRY OF THE UCAYALI RIVER, PERU

by

Kristin R. Dauer

B.S. in Civil Engineering, University of Pittsburgh, 2012

Submitted to the Graduate Faculty of

the Swanson School of Engineering in partial fulfillment

of the requirements for the degree of

Master of Science

University of Pittsburgh

2015

UNIVERSITY OF PITTSBURGH

SWANSON SCHOOL OF ENGINEERING

This thesis was presented

by

Kristin R. Dauer

It was defended on

December 11, 2014

and approved by

Jorge D. Abad, PhD, Assistant Professor, Department of Civil and Environmental Engineering

Daniel J. Bain, PhD, Assistant Professor, Department of Geology and Planetary Science

Xu Liang, PhD, Professor, Department of Civil and Environmental Engineering

Thesis Advisor: Jorge D. Abad, PhD, Assistant Professor, Department of Civil and Environmental Engineering

DYNAMIC AND STATIC CHARACTERIZATION OF THE PLANIMETRY OF THE UCAYALI RIVER, PERU

Kristin R. Dauer, M.S.

University of Pittsburgh, 2015

The Ucayali River, one of the largest rivers in the Peruvian Amazon, is one of the most dynamic rivers in the region. The Upper Ucayali River is a single-thread, meandering river, while the Lower Ucayali has multiple threads. Before being able to answer complex questions such as if the planform characteristics of Ucayali River are affected by climate change or land use change, the river itself needs to be characterized. The river can be characterized both in terms of the planform and morphometrics. I have developed a toolbox to facilitate the calculation of static planform statistics on meandering rivers, and have calculated some basic parameters of a reach of the Ucayali, including wavelength, amplitude, and orientation of bends. In order to understand the morphodynamic processes on the Lower Ucayali River, which has multiple threads, I have conducted a case study of one reach where two cutoffs have occurred in recent years, and where a third may soon happen. The study includes a temporal analysis using satellite imagery, hydrodynamic and morphodynamic field measurements and a two-dimensional Reynolds Average Navier Stokes (RANS) model, in order to predict how and when the cutoff may occur.

TABLE OF CONTENTS

LIST OF FIGURES

1.0 INTRODUCTION

The Amazon River, with its source in Peru, is one of the largest rivers in the world based on discharge (*Latrubesse et al.*, 2005). Over recent decades there have changes in the climate of the basin, and in some locations, activities such as deforestation and dam construction (*Holeman*, 2010; *Patel*, 2013). In the Upper Amazon Basin, there are fewer of the drastic land use changes that are seen elsewhere in the basin, but still, measurements of runoff, discharge, and rainfall indicate that the climate patterns have been changing as far back as the 1970s (*Espinoza et al.*, 2009a). If changes in climate and land use, which influence factors such as runoff and sediment discharge, have been shown to be related to changes in sedimentation in relatively smaller river systems in Europe and Asia (*D.E. Walling*, 1996; *W.B. Langbein*, 2013), changes in the planform characteristics of a large river in the Amazon Basin over the short term due to changes in climate or land use may be detected.

The Ucayali River, one of the largest rivers in the Upper Amazon Basin, at 1,465 km long and with an average discharge of 14,000 m^3/s, is one of the most dynamic rivers in the region. The Ucayali River is characterized as a white water river, with its flow originating in the Andes and its foothills, it carries relatively large amounts of sediment (*Dumont*, 1991). The amount of sediment in a river and how it is transported are of interest because the sediment affects how the river migrates over time (*Abad and Garcia*, 2009). Understanding how the river moves can have implications such as being able to predict or prevent a cutoff in a meander bend, which could have impacts such as isolating villages and changing inundation and sediment deposition regimes (*Coomes et al.*, 2009). *Lathrap* (1968) divides the Ucayali into three sections: the Upper Ucayali Basin is located in the Andes mountains and contains the Urubamba and Tambo rivers, the two rivers that join in Atalaya (A in Figure 1), Peru to form the Ucayali River. The Central Ucayali continues through the Subandean foothills

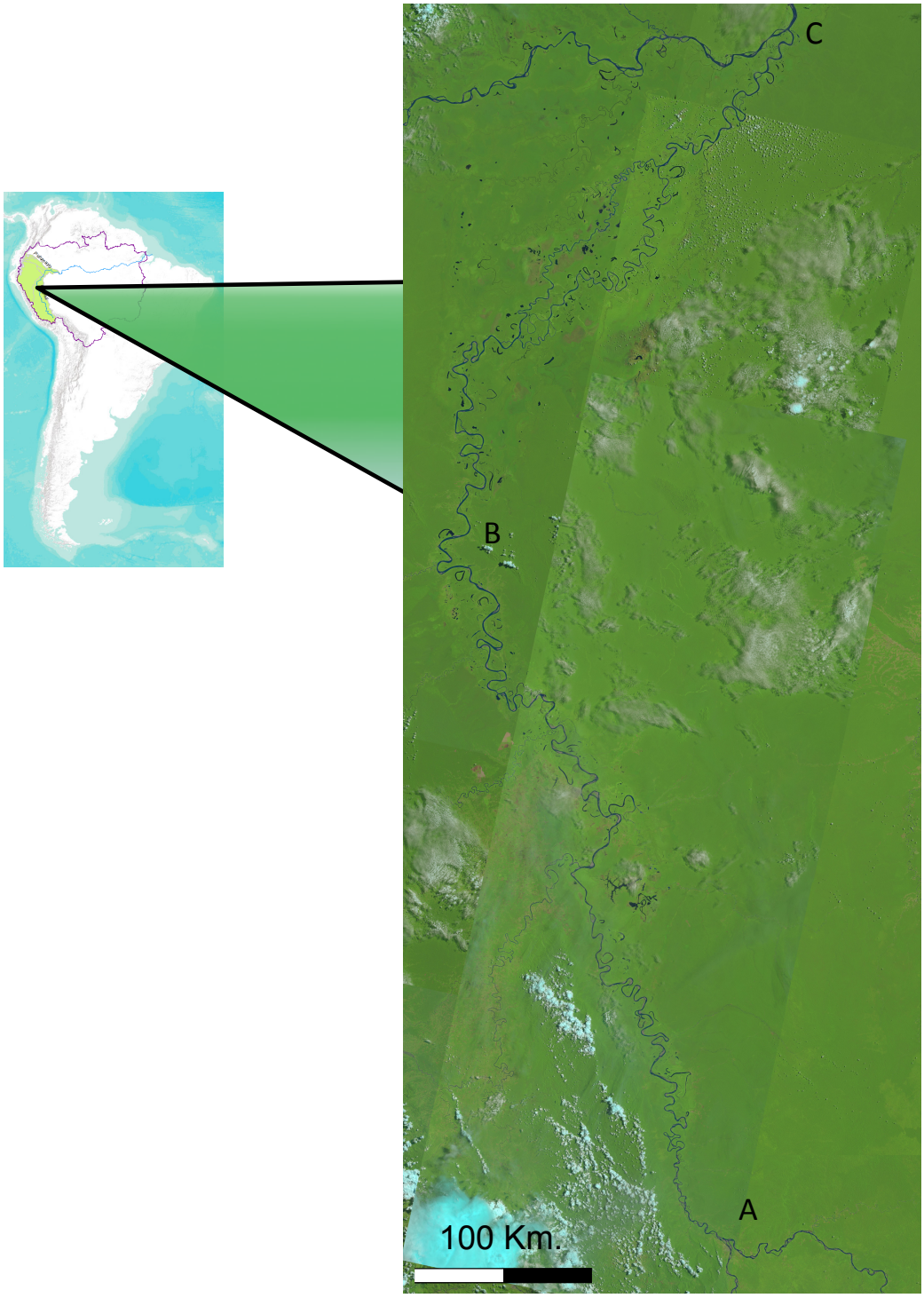

Figure 1: The Ucayali River, flowing from Atalaya in the south (A) to the beginning of the Amazon River (C).

until it is confined on both sides by the Contamana Mountains (B in Figure 1), where it enters the Ucamara Depression and the wider valley of the Lower Ucayali begins and flows until the confluence with the Marañon River, where the Amazon River begins (C in Figure 1).

Some of the factors that can impact the morphodynamics of a river include the surrounding geologic features and the climate. Over the length of the Ucayali River, these factors vary. *Lathrap* (1968) characterizes the Central Ucayali Basin as a broad structural depression with the streams incised into weathered alluvial deposits and with prominent bluffs, 30 to 40 feet high along the edges of the floodplain. The Ucamara Depression, in the Lower Ucayali Basin, is bounded on the north by the Marañon River, on the west by the Samiria River, and on the south and east by a morphostructural boundary formed by the Tapiche fault and the edge of the Iquitos geanticline; the depression is subsiding and, as a result, is characterized by large swamps (*Dumont*, 1991). These geological features are also of interest because they may show places where the migration of meandering rivers is confined. Data collected by *Dumont* (1991) shows that during the period of high flow, the water level rises about $11m$ at both the foothills in the Central basin and in Iquitos, about 70 miles downstream of the mouth of the Ucayali, while in the Ucamara Depression, the water level only changes by about 2 m. This difference in hydrology between the parts of the basin may result in different morphodynamic characteristics.

In the Lower Ucayali Basin, the amount of monthly rainfall varies much less than in other areas of the Amazon. There is relatively high rainfall in this region throughout the year, with an annual total between 2,000-3,000 mm. In the Upper and Central Ucayali Basin, however, there is relatively higher variation throughout the year, but less total rainfall in general (*Espinoza et al.*, 2009b). In addition to seasonal changes, inter-annual variations in rainfall, such as those caused by El Nino-Southern Oscillation (ENSO) play a prominent role in the variations in hydrology. Both the positive and negative phases of this phenomenon can impact the discharge, causing the flow to decrease or increase, respectively. When these events are more severe, they can lead to events such as a very low river stage, which can result in the death of aquatic wildlife (*Bodmer et al.*, 2011), or a very high flow, which can alter the course of the river through processes such as avulsion (*Coomes et al.*, 2009).

Currently, there are plans in place to build dams in the Upper Ucayali Basin, along with dredging of the Ucayali River in order to facilitate the movement of large, industrial vessels (*Castello et al.*, 2013). Before being able to analyze if the Ucayali River is affected by climate or land use change, it is first necessary to characterize the planform of this long river, both in terms of its geometry at a fixed point in time (static characteristics) and also how the geometry of the river changes over time (dynamic characteristics). Calculating static characteristics manually is time consuming and can involve arbitrary judgement. In Chapter 2, I describe a toolbox that I have developed to facilitate the calculation of static planform statistics on meandering rivers. In order to understand the dynamic characteristics of the Ucayali River,I look at a process that has a dramatic effect on the planform of a meandering river, the meander bend cutoff. Chapter 3 uses a case study on a portion of the Lower Ucayali River to analyze how the river has moved over time and how meander bend cutoffs occur in this portion of the river, which has multiple threads. The goal is to look at two methods for characterizing the river, focusing on one reach in the Central Ucayali and one in the Lower Ucayali.

2.0 MSTAT: A TOOLBOX FOR PLANFORM CHARACTERIZATION OF MEANDERING STREAMS

2.1 INTRODUCTION

Human activities and development projects continue to have an impact on ecosystems, including riparian zones. Factors such as increases in runoff, urbanization within a river basin and the construction or removal of water control structures can all affect the characteristics of streams. Some of these effects can be seen in the morphodynamics of the plan or bed forms. The primary goal of this research was to develop a tool to interpret and analyze stream centerline data. This computer program, called mStat, will allow more effective performance of multi-disciplinary projects such as restoring channelized streams to more natural, stable conditions. The toolbox accepts digitized river centerline data and river width as inputs, calculates a mean centerline using wavelet filter analysis, and computes meander bend characteristics such as sinuosity, length, orientation, wavelength, and amplitude. In addition, the toolbox uses wavelet analysis to compute additional river bend properties such as angular amplitude from stream-wise coordinates and curvature. Currently, mStat is coded using Matlab, but I am planning to incorporate it into the River Restoration Platform, RVRMeander (www.rvrmeander.org).

2.2 METHODS AND MATERIALS

The initial step in this project was to gather spatial river data to develop and test the toolbox computation processes. Natural meanders that did not exhibit significant effects

from urbanization or modifications for navigation were chosen from locations in the southern United States, South America, and Canada. Satellite data were collected for 13 river reaches, with 5 different years of data for each stream. These data were digitized into stream-wise and Cartesian coordinates using AutoCAD Map 3D and ArcGIS 10.1. Then, code was developed in MATLAB 2013a to perform analysis on the input data. This code was integrated into a Graphical User Interface (GUI) to allow the user to easily see, interact with, and interpret the data processed by the toolbox. The GUI accepts input from the user, plots the river centerline data, plots bend limits and inflection points, and displays statistical results for basic river features. The user can calculate river statistics using both planar geometry and wavelet analysis.

2.3 THEORY/ CALCULATION

After opening the program interface, the user is required to input a single river centerline in (x,y) Cartesian coordinates as an ASCII file and enter the mean river width in meters. The toolbox then processes the centerline point data so that it can be used for calculations in the "geometry" section. The processed centerline data are then analyzed to define the bends in the "bends" section, the processed bend data are analyzed in the "statistics" section where characteristics of the bends are determined, lastly the data are plotted in the graphical user interface (GUI) window so the user can interact with it.

2.3.1 Geometric Processing

The centerline data that the user inputs is in Cartesian coordinates and not necessarily equally spaced, but for calculations the data should be equally spaced at a distance of one channel-width (*Gutierrez and Abad*, 2014; *Hooke*, 1984; *Legleiter and Kyriakidis*, 2006). In addition, having the ordinates of the data in streamwise distance, s, facilitates the processing and calculations. A method developed by *Legleiter and Kyriakidis* (2006) and described by *Gutierrez and Abad* (2014) was used in a function called "getxyresampled" that processes x,y

centerline points by obtaining equally spaced points and obtains the streamwise ordinates and curvature for these equally-spaced points. The equally spaced points are then processed by the Principal component analysis(PCA)-wavelet filter to obtain the mean centerline as described by *Gutierrez and Abad* (2014). As explained by *Gutierrez and Abad* (2014), the mean centerline (MC) provides a description of the river for the medium-term between the instantaneous time frame and the geologic time frame. This mean centerline, therefore approximates the centerline of the active meander belt. The points of intersection between this MC and the equally-spaced river centerline are also calculated in this section as an input to the "bends" section. Lastly, the points of maximum curvature are determined from the curvature data that are an output of the "getxyresampled" function.

2.3.2 Meander Bend Definition

The output from the "geometry" section is used as an input to the "bends" section, where the bends are defined and some of the attributes are assigned to the meander bends. First, each meander bend is defined as starting and ending where the river centerline intersects the MC (see Figure 2). A meander bend is commonly defined as a section of the river between two inflection points, but in this particular case, with real centerline data that are digitized by the user in terms of x,y points, there may be noise in the centerline signal, even after processing to equally space the data, that can lead to erroneous definitions of bends. The intersection of the centerline and the MC closely approximates the inflection points that define the bends, therefore these intersection points are used instead of the inflection points since they are not as sensitive to noise in the centerline signal. If there are centerline points before or after the first bend, they are trimmed at this time, so that only complete bends are analyzed. The centerline data are then organized in a matrix, where each row contains data for a different bend, specifically the points that define the beginning and end of the bend and any points of maximum curvature located in the bend.

Once organized, the bends are characterized broadly as either simple or compound bends, where the simple bends have only one point of maximum curvature and compound bends have at least two points of maximum curvature in the bend. From here, the simple bends are

characterized as either upstream-oriented, downstream-oriented or symmetric. If the point of maximum curvature is located less than half the distance between the beginning and end of the bend, along the stream centerline, it is upstream-oriented. If it is greater than half the distance between the beginning and end of the bend, then it is downstream-oriented, and if it is located halfway between the beginning and end, then it is symmetric.

2.3.3 Calculation of Characteristics

Now that the data are organized into bends, the characteristics can be calculated for each bend. The sinuosity is calculated by dividing the arc-length of the bend by the Cartesian distance. The wavelength is calculated by measuring the Cartesian distance between the beginning and end of the bend. The amplitude is calculated by finding the orthogonal distance between the point of maximum curvature and a straight line connecting the beginning and end points of the bend. In the case that there are multiple points of maximum curvature in a bend, the amplitude is calculated at each of the points of maximum curvature and the largest value is used for the bend amplitude.

2.3.4 Plotting and Interacting with the Data

After the data have been processed, it is plotted in the GUI window. The user can see the centerline and the MC plotted, along with the intersection points that define the bends and the points of maximum curvature plotted together in one window. In addition, the bends are labeled with the bend indentification numbers and have letters describing the shape: "C" for compound, "US" for upstream-oriented, and "DS" for downstream-oriented. The user can zoom and pan to see a specific part of the river, and can select a bend from a list and press the "bend statistics" button to display the characteristics for that particular bend. Pressing the "river statistics" button populates a table showing the characteristics for all of the bends. Another button in the main window is the "wavelet analysis" button. This plots the data after it has undergone the wavelet analysis. For more information regarding the wavelet analysis, please refer to *Gutierrez and Abad* (2014).

2.4 CASE STUDY: UCAYALI RIVER

A section of the central Ucayali River was selected for analysis because it has only a single channel in the selected section. Even over the reach selected for analysis, the class of the river varies from class C at the upstream portion and class D at the downstream portion, according to the Brice classification system (*Gutierrez and Abad*, 2014). The data used in this analysis, from *Gutierrez and Abad* (2014), depict the centerline of the channel in the year 2005.

The analysis shows that on this portion of the river, the sinuosity of meander bends ranges from 1.0 to 1.7. The wavelengths range from 2.1 km to 12.7 km (1.9-11.3 mean channel widths), while the amplitudes range from 10.6 to 30.9 km (9.4-27.5 mean channel widths). These characteristics can be used to classify the type of bend.

Of the 25 meander bends on this reach of the Ucayali River, 21 were simple, only having one point of maximum curvature. 11 of the simple bends were downstream skewed, while 10 were upstream skewed. 4 bends were classified as compound, having multiple points of maximum curvature in the bend.

2.5 DISCUSSION

While several authors have developed computer code that can be used to perform similar tasks to this program, mStat is a user friendly tool that can aid designers and students in statistical analysis of meandering rivers. The GUI presents an effective teaching tool for instructors as well as an overview of key statistics for designers and consultants. This information is useful for designing stream restoration or planning river crossings. In this article, mStat and digitized riverbank data were used to calculate bend characteristics on a portion of the Ucayali River. These characteristics were verified by hand calculation and could be used to classify the river reaches as confined meanders, free meanders, or some combination of these two. The toolbox could benefit from adding a component to analyze dynamic characteristics in addition to these static characteristics.

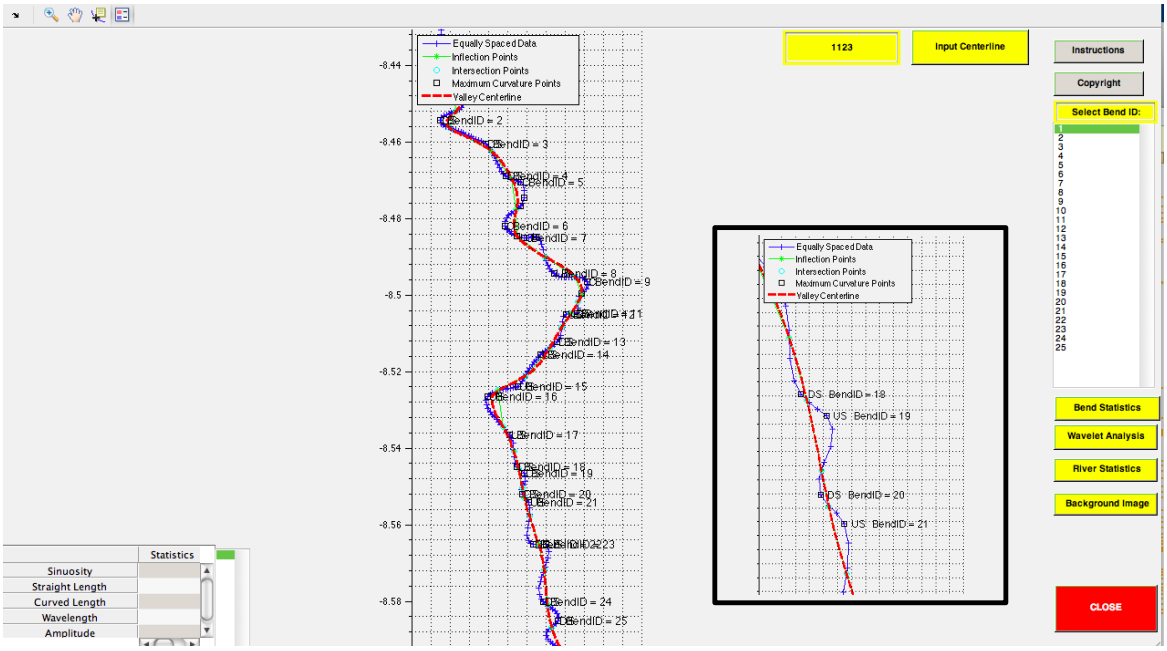

Figure 2: mStat Main Window, Showing a Portion of the Ucayali Centerline After Analysis.

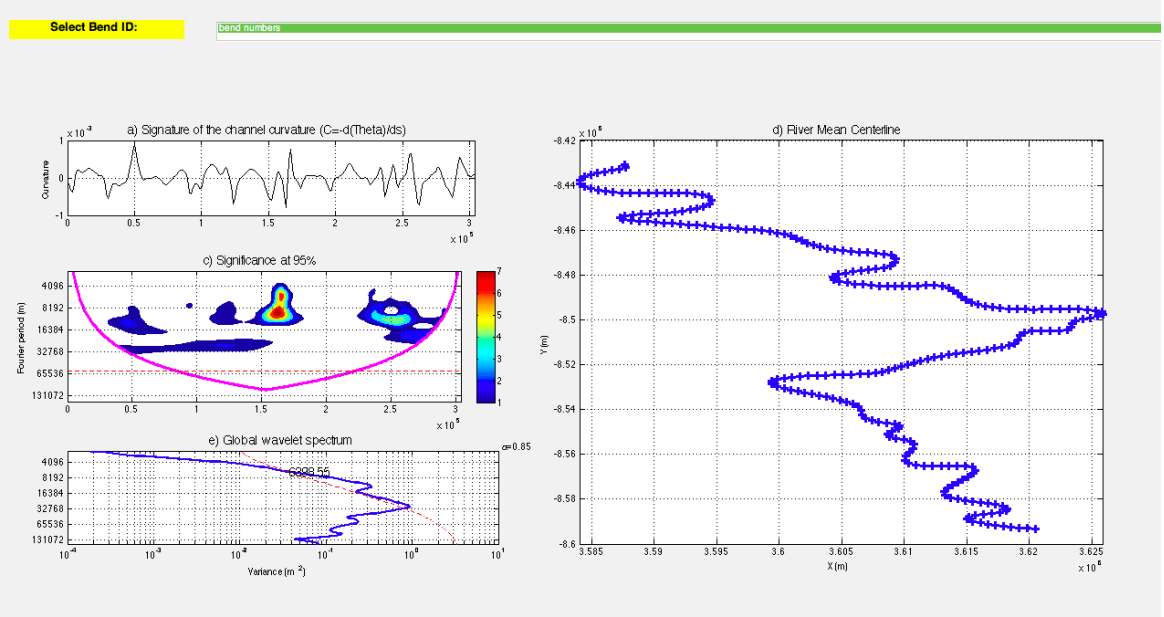

Figure 3: Wavelet Analysis of the Ucayali River. The first plot (a) in the wavelet statistics window plots a signal showing the curvature along the channel centerline. The next plot (b) shows the frequency of different wavelengths along the channel centerline, and the last plot (c) shows the global wavelet spectrum.

2.6 CONCLUSIONS

The current version of mStat characterizes the bends as simple or compound, based on the number of points of maximum curvature, but the characteristics calculated above could be used to give a more refined characterization of the bend type, such as the classifications put forth by *Brice* (1974). This Toolbox was applied to the Ucayali River, one of the rivers that form the Amazon River. While this toolbox is useful for calculating static characteristics of a stream, it does not have the capacity to analyze dynamic properties. In the near future, I am planning to have mStat as part of the River Restoration Toolbox RVR Meander (www.rvrmeander.org).

2.7 ACKNOWLEDGEMENTS

The authors would like to thank Dr. Legleiter for the use of his tools for processing centerline data. Thanks to Brian Hone and Ronald Gutierrez for helping out during the initial stages of the toolbox.

3.0 JENARO HERRERA: ANALYZING PLANFORM DYNAMICS AND PREDICTING MEANDER BEND CUTOFFS

3.1 INTRODUCTION

The Ucayali River is a large, meandering river in the Upper Amazon Basin that drains an area of 360,000 km^2 (*Guyot et al.*, 2007; *Guyot*, 2007). Draining the Andes, it carries one of the highest suspended sediment loads of any of the tributaries to the Amazon (*Schumm et al.*, 2000; *Goulding et al.*, 2003; *Puhakka et al.*, 1992; *Wittmann et al.*, 2011). In terms of planform migration, the Ucayali is one of the most active rivers in the Upper Amazon Basin, and oxbow lakes and chute cutoffs are common features along the river (*Parssinen et al.*, 1996; *Guyot*, 2007; *Lathrap*, 1968; *Puhakka et al.*, 1992). Past studies have calculated the migration rate at the apex of a meander bend to be 60-80 m/year, with maximum rates reaching 150 m/year, while migration on reaches between the apex and inflection point of a meander average around 25 m/year (*Schumm et al.*, 2000; *Puhakka et al.*, 1992; *Guyot*, 2007; *Lamotte*, 1990). This dynamic river has been central to the societies that have populated it for thousands of years, due to the fertile soils in the floodplain, fishing, and the connectivity that it provides between communities; the river still plays a vital role today for these same reasons, as regional roads are minimal — ninety percent of cargo and passenger traffic in the department containing the lower Ucayali River travels on the fluvial network (*Lathrap*, 1968; *Salonen et al.*, 2011). However, unlike man-made transportation networks, the distance of travel between two points on the Ucayali River changes over time, due to migration of the river and the formation of cutoff channels. The cutoff process plays an important role in meandering river dynamics by reducing the complexity of a particular reach and also by acting as a noise that changes the dynamics of the river on a whole; it is important

for maintaining the steady-state of a river (*Frascati and Lanzoni*, 2009; *Camporeale et al.*, 2008). There are two types of cutoff processes that can occur on a meandering river. In neck cutoffs, the sinuosity and tortuosity of the bend become so high that the water crosses the narrow neck, resulting in the two limbs effectively colliding (*Gagliano and Howard*, 1984; *Camporeale et al.*, 2008). In chute cutoffs, which typically occur in wide channels with large curvature, high discharges, high gradients, and poorly cohesive, weakly vegetated banks , a new channel is cut across the neck of a meander bend during floods and reduces sinuosity (*Howard and Knutson*, 1984; *Gay et al.*, 1998; *Howard*, 1996; *Camporeale et al.*, 2008); *Frascati and Lanzoni* (2009) specify that a chute cutoff channel is relatively long, similarly *Lewis and Lewin* (1983) only consider cutoffs that occur at a distance greater than one channel-width as a chute cutoff, while *Gay et al.* (1998) consider any process in which a new channel is incised as a chute cutoff. I will follow the definition of chute cutoff used by *Gay et al.* (1998). Predicting chute cutoffs remains an unresolved problem, but it may be an important process for long-term sediment flux (*Frascati and Lanzoni*, 2009; *Zinger et al.*, 2008). After a cutoff occurs, oxbow lakes form if the old channel becomes closed by sedimentation (*Frascati and Lanzoni*, 2009; *Hudson and Kesel*, 2000). While a cutoff may reduce travel time for some people using the river network, it can also lead to increased flooding downstream of the cutoff and isolation of towns from their source of fishing, sites for planting crops, and the fluvial transportation network (*Abizaid*, 2005; *Coomes et al.*, 2009). From observation of satellite imagery, two cutoffs on the Lower Ucayali River have occurred in the past fifteen years, and one more meander bend appears to be close to cutoff. I aim to predict when this third cutoff will occur by using both temporal analysis of Landsat images and a numerical model paired with field measurements.

3.2 THE FIELD SITE: JENARO HERRERA

The town of Jenaro Herrera (population 5,100) is located on the apex of a meander bend along the Ucayali River (4.909448S, 73.670120W) (*Instituto Nacional de Estadistica e Informatica*, 2007). The main industry in this town is agriculture, followed by fishing (*INICTEL*

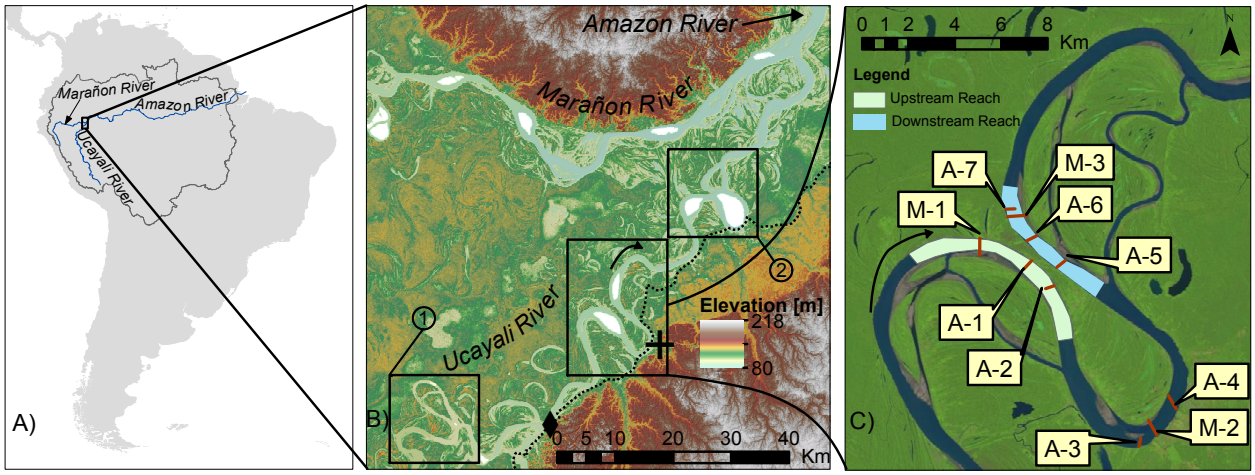

Figure 4: A) The gray outline delineates the Amazon River Basin. The Ucayali and Marañon River, which form the Amazon River are shown in blue. Base map from ESRI. Hydrologic data adapted from *Muller et al.* (1999); *Seyler et al.* (2009). B) Digital Elevation Model of Lower Marañon Basin. The confluence of the Marañon and Ucayali is shown in the upper right corner, where the Amazon River begins. Locations 1 and 2 are an oxbow lakes located upstream and downstream, respectively, of the Jenaro Herrera Site. The arrow along the Ucayali River indicates the direction of flow. The diamond marker along the Ucayali River indicates the location of the Requena gaging station. The plus marker indicates the location of the Jenaro Herrera municipality (−73.668658, −4.903989). The dotted line indicates the Tapiche fault at the edge of the Brazilian craton (*Schumm et al.*, 2000; *Pittman and Salgado*, 1999). C) The locations of the aDcp transects that were taken in 2013. Transects that begin with "M" were taken in May, while those labeled with "A" were taken in August. For the water stage at the Requena station on the dates when the measurements were taken, see Figure 5. The arrow indicates the direction of flow (Landsat ETM+ image from August 28, 2013).

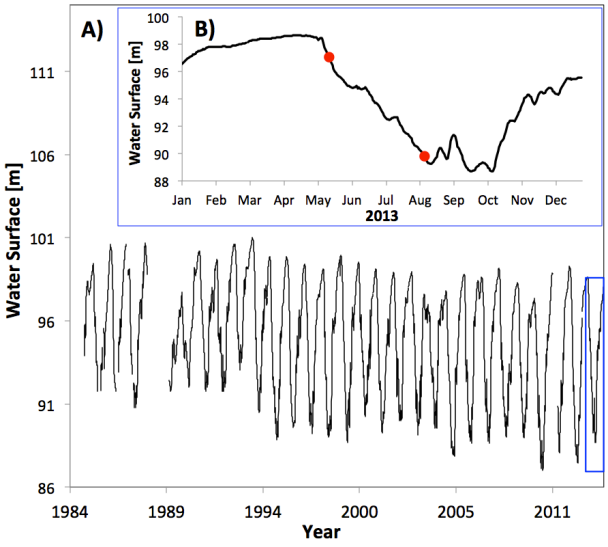

Figure 5: The water level in meters at the Requena gaging station (see Figure 4), A) from 1984 to 2014. The gray box encloses the measurements from 2013. B)Water level measurements at Requena during 2013. The dots indicate the dates of field measurements.

- *UNI, Dirección de Proyectos y Transferencia de Conocimientos*, 2009). There is also a biological research station located here where national and international scientists study the ecology of the Amazon rainforest. The primary transportation connection between this town and other cities in the region is by the Ucayali River. The meander bend where Jenaro Herrera is located has been narrowing at the neck over the past decades, and now the distance between the two limbs is less than 500 meters (Figure 4). If a cutoff were to occur along this meander, this could cause difficulties for transportation as well as the economy. As observed in Figure 4, the Ucayali River is not a purely meandering river, instead it is a transitional channel from meandering to anabranching channel. Daily water surface elevation data is from the Requena gaging station on the Ucayali River for the period of 1983 to 2013 (Figure 5), managed by the Peruvian National Meteorology and Hydrology Service, SENAMHI, (www.senamhi.gob.pe). Gaps show where no data was available, most notably from May 1988 to August 1989.

3.3 TEMPORAL MIGRATION ANALYSIS

In order to gain an understanding of channel migration and cutoff processes in this reach of the Ucayali River, I performed a temporal analysis for two of the meander bends that cutoff in recent years on the lower Ucayali. Landsat TM images, which have a resolution of 30 meters (glovis.usgs.gov), were used for the temporal analysis. Planform characteristics have been calculated for these bends in order to determine if there are any common factors in the cutoff processes. This analysis answers the following questions: What were the planform characteristics in these channels as they approached cutoff (sinuosity, distance between limbs, migration rates, etc.)? What were the mechanisms for cutoff? How long did it take to complete the process, and what were the hydrologic conditions during these years? Sinuosity is defined as the ratio of the channel length to the valley length (*Ferguson*, 1977). This was calculated using a toolbox called mStat.

Figures 6, 7, and 8 show the changes in the channel over five year periods, except for the first sequence in each figure (1985-1988), which is only three years due to limited imagery available before 1985. In all of the figures, blue represents areas where the river has been consistently located over the five year period. Green represents deposition by the channel, or areas that the river has abandoned since the first year of the comparison. Red areas show erosion, or areas that the river has migrated into by the end of the five-year period. However, a significant difference in water level in the two images being compared can make it appear that there has been more change in the channel than has actually occurred. In order to avoid this, Landsat images from the low season of July through September have been collected, and when cloud-free images were not available during this period, images from the transitional period between the high and low season were used instead. However, in 1993, the water stage was higher than typical (see Figure 5). This is especially true during the typical low season. Rainfall data collected at the nearby Tamshiyacu station shows that the average monthly rainfall during 1993 was among the highest of the study period, especially from September through November, which is typically the drier season (*Espinoza et al.*, 2013). Therefore, the total area eroded between 1988 and 1993 and the total area deposited between 1993 and 1998 are likely exaggerated in the temporal analysis figures.

3.3.1 Characteristics of Upstream and Downstream Migration Processes

The cutoff upstream of the Jenaro Herrera bend (Location 1 in Figure 4B) took place between September and December 1990, as observed from Landsat images. The meander bend became very elongated before the cutoff occurred and a secondary channel like a chute cutoff was present in the bend (Figure 6). The upstream limb of the bend had a high sinuosity, and proceeded to collide into the downstream limb, which had a low sinuosity reach and was migrating at a lower rate. This collision created a connection with a width approximately equal to the main channel width. In a Landsat image from April 1991, the color of the water in the new and old channels are different, indicating that the sediment concentration is different in these two portions of the channel and the water is flowing through the new channel and has largely bypassed the old channel. By September 1995, the old channel is only connected by a narrow channel. After the old section of the bend was abandoned, the new bend began a process of downstream translation, as expected in the early stages of a meander bend (*Brice*, 1974).

The water levels on the lower Ucayali River from December 1989 to April 1990 were the lowest recorded for this transitional-high stage season in the period of 1984 to 2013. However, following this period of unusually low water levels, some of the highest water levels for July and August during the study period occurred, and the rest of the year showed higher than average water levels.

The beginning of the downstream cutoff (Location 2 in Figure 4B) is evident in the Landsat imagery beginning around July through December 1996, when a small channel with a width about one-ninth of the main channel width is incised on the downstream side of the meander loop, where the floodplain separated the two limbs by a distance of approximately 300 meters, or about one-third of the main channel width (Figure 7). By June 1997, the cutoff is complete, and the cutoff channel is approximately at full-channel width. The bifurcation of the cutoff channel is near the bifurcation of secondary channel on the downstream reach of the bend. The path of the river does not only change at the location of the cutoff, but also just downstream. After the cutoff channel has formed, the water downstream of the cutoff is rerouted through the secondary channel, a path that reduces the sinuosity.

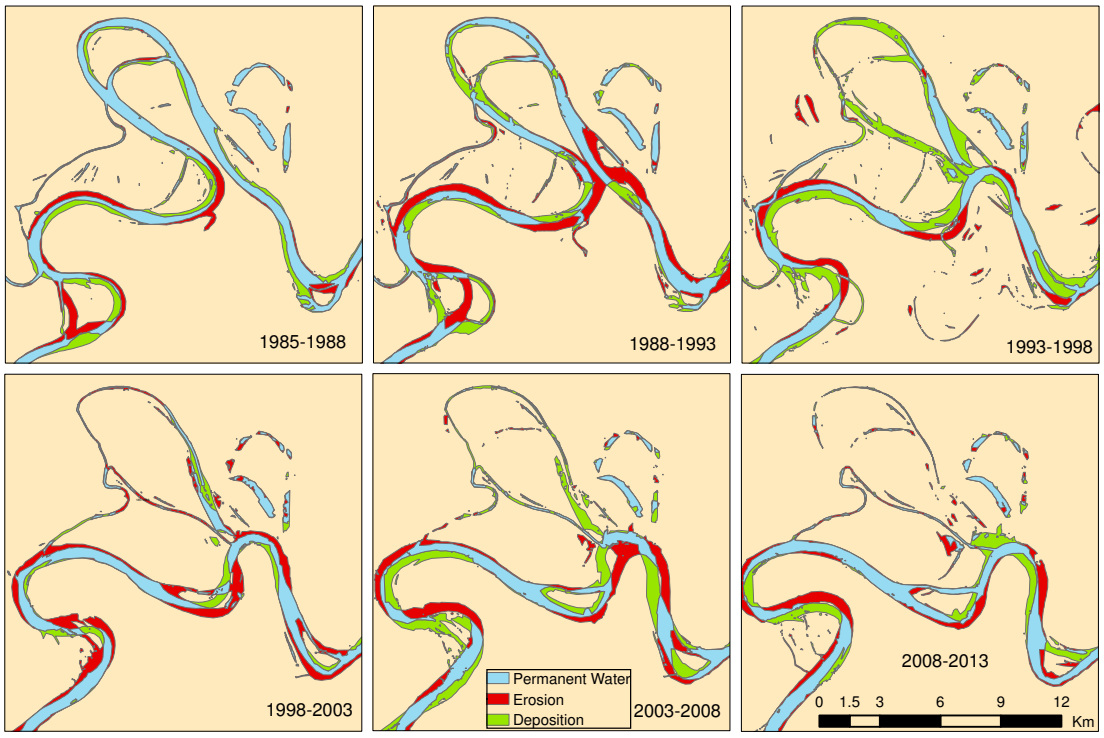

Figure 6: Migration of the Ucayali River Upstream of Jenaro Herrera (Location 1 in Figure 4). Each image was created using two Landsat images, one from each of the two years listed in the corner. For example, the image with "2008-2013" was created using an image from 2008 and one from 2013. The blue portions of the channel indicate where the river has been for the whole time period. The green indicates areas of deposition, where the channel was at the beginning of the period, but abandoned by the end of the period. The red areas indicate erosion, areas into which the channel has moved into by the end of the period. All of the images compare a period of five years, except for the first one, 1985-1988, which only compares a period of three years because of a lack of images available before 1985.

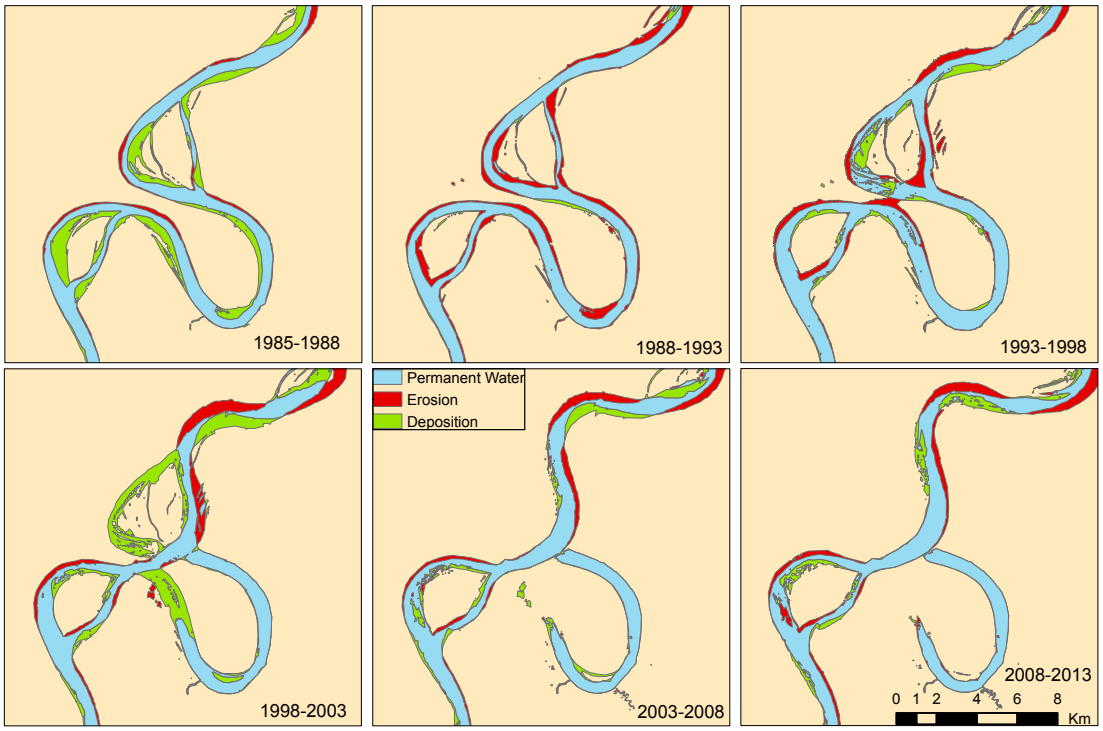

Figure 7: Migration of the Ucayali River Downstream of Jenaro Herrera (Location 2 in Figure 4). See Figure 6 for further description.

The high season of 1996 (from late January through June) had higher than average water levels and some higher than average episodes in the transitional stage from October through December, but did not vary from the average by more than 1.7 meters. The cutoff process at the downstream bend may be explained by the mechanism described by *Gay et al.* (1998), where a channel is incised from the downstream side of the loop over multiple flood seasons. Some of the highest water levels during the period of record, exceeding the daily average by more than 4.5 meters at some points, were during 1993 and 1994, where 1993 showed some of the highest recorded stages for almost the entire year and 1994 had some of the highest recorded stages from the peak through the transition into the low season. The river stages during the high seasons of 1995 and 1996 were lower than in 1993 and 1994, but were still higher than average. It appears that there was a narrow channel across the loop in the image from June 21, 1994; in 1996, the new channel appears on the downstream end of where this same channel was located. From the Landsat images, both cutoffs appear to have occurred as the water level is transitioning from the seasonal low to high. By the end of the high water season, the new channel has developed to full width and has become the preferred flow path. The upstream cutoff appears to have occurred during a year with unusually low flows in the high season and unusually high flows in the low season. This quick transition may have led to less vegetation in the floodplain, facilitating the collision of the the two reaches to form a new channel. The downstream cutoff, however, was likely formed over a longer time period, based on the process described by *Gay et al.* (1998), but once the new channel was large enough to be seen clearly in the Landsat imagery (resolution of 30 meters), the cutoff was completed in the same year.

3.3.2 Temporal Analysis at Jenaro Herrera Site

The meander bend located near Jenaro Herrera does not show as much activity as the two bends where meander cutoffs occurred, despite its high sinuosity. This bend appears to cross a fault and the reach near the apex of the meander bend, which is about 10 km long, borders the Upper Nauta and Ucamara formations instead of just alluvial deposits (*Pittman and Salgado*, 1999). The lower Ucayali River is near the Brazilian Craton with an escarpment

that borders the downstream portion of the Jenaro Herrera bend (*Schumm et al.*, 2000; *Pittman and Salgado*, 1999). This structure confines part of the bend, preventing it from eroding the banks at the rate seen in nearby bends. The loop on the upstream side of the Jenaro Herrera bend has become more rounded over the past years, with a larger radius of curvature, and migrated downstream towards the downstream loop. The downstream loop has also migrated towards the upstream loop at its apex, but to a smaller degree; therefore, the upstream portion is migrating towards the downstream portion faster than the downstream portion is migrating away from the upstream portion, indicating the possibility for a cutoff similar to the one at Location 1.

3.3.3 Migration rate analysis of Jenaro Herrera bend

Schumm et al. (2000) estimated a migration rate of 60 m/year at the apex of meanders in the lower Ucayali River, and estimated that it would take 100 to 200 years for a meander loop to form. I calculated the migration rates for each year using the Planform Statistics Tool from the National Center for Earth-Surface Dynamics (*Lauer*, 2006). *Frias et al.* (In Review) describe the methodology. Migration rates were calculated for the reaches upstream and downstream of Jenaro Herrera (Figure 9). Average migration rates of the outer banks were calculated for each year in the period of study by using the bank lines from the current and previous year. The average migration rate for a reach was calculated using Equation 3.1, where s is the streamwise distance and m is the distance of migration in meters. For the years 1986, 2006, and 2012, quality images were not available in the low season, so the migration rates are calculated using the year before and after the missing year, and dividing the migration by 2 to get the migration per year.

$$\frac{\sum_{i=1}^{n}(s_{i+1} - s_{i-1})m_i}{s_n - s_1 + s_{n+1} - s_0} \tag{3.1}$$

The average migration rates were 28 m/year and 17 m/year on the upstream portion and downstream portion, respectively. No increasing or decreasing trend was observed in the migration rate over the period of study. At its most narrow point, the floodplain inside of the loop is 450 m wide. Assuming that the two reaches continue to migrate at their current rates, this would mean they could collide and form a cutoff in approximately 10 years.

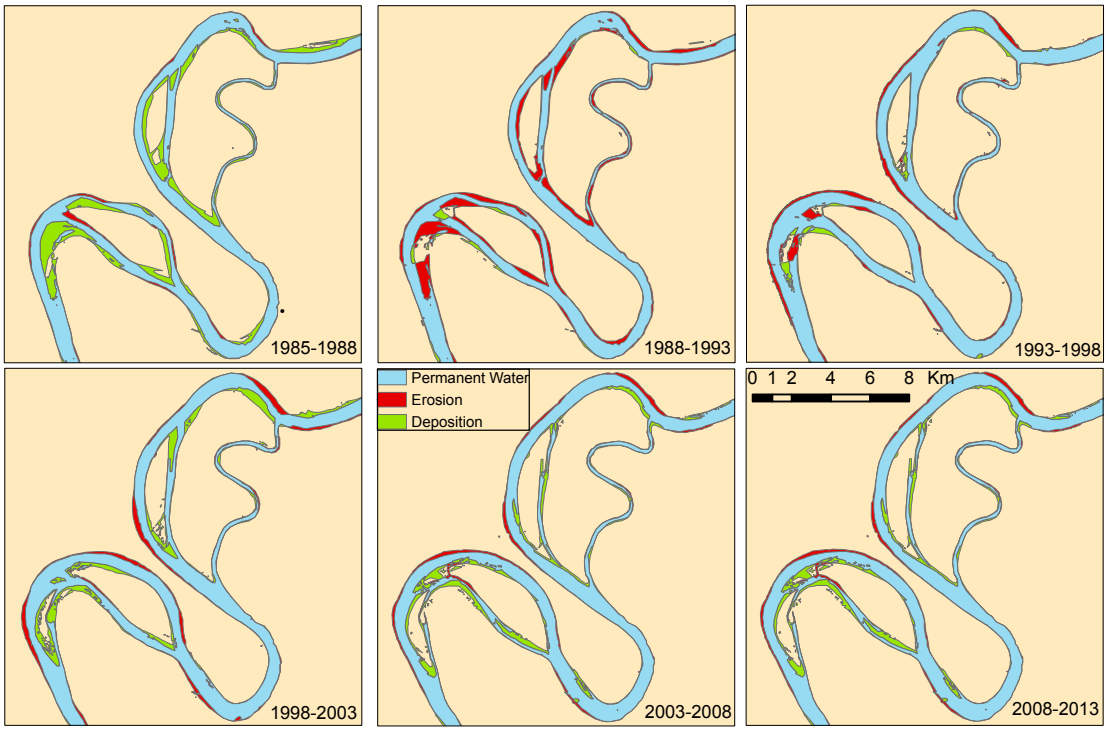

Figure 8: Migration at Jenaro Herrera. See Figure 6 for further description.

3.3.4 Discussion of the problem

As previously discussed, there are multiple mechanisms for a cutoff channel to form. Aside from the two channels colliding to form a cutoff, it is also possible that a cutoff could occur due to the formation of a channel inside of the meander bend over time. There is a headcut that is visible during the high or transitional periods of the year in several images from 1993 through 2014. It is possible that this could develop into a chute cutoff channel over time, similar to the channel that formed in the bend downstream (Location 2). This depends on the hydrologic conditions in the upcoming years, as well as the terrain, vegetation, and lithology and can be challenging to predict (*Frascati and Lanzoni*, 2009; *Camporeale et al.*, 2008). In addition, cutoff channels can form in the swales where the channel previously migrated. The bend at Jenaro Herrera has a similar shape to the bend in Figure 7. It is possible that upon the formation of a cutoff channel, the water downstream could be routed through the secondary channel labeled "C3" in Figure 10, in order to reduce sinuosity, as happened at the downstream cutoff (Figure 7).

3.4 THE FIELD MEASUREMENTS 2012-2013

Field measurement campaigns were carried out in May and August of 2013, in order to obtain measurements during both the high and low seasons (see Figure 5 for hydrograph).

3.4.1 Hydrodynamics

Velocity measurements were taken at transects in the bend during both field measurement campaigns using an acoustic Doppler current profiler (aDcp) and processed using the Velocity Mapping Tool (VMT) (*Zinger et al.*, 2008; *Parsons et al.*, 2013). The locations of the measurements are shown in Figure 4C, where the letters "M" and "A" indicate in which month the measurement was taken. The velocity profiles at these cross-sections are shown in Figure 11 for May and Figure 12 for August. The contour plot indicates the velocity magnitude, while the vectors show the direction and velocity magnitude of the secondary

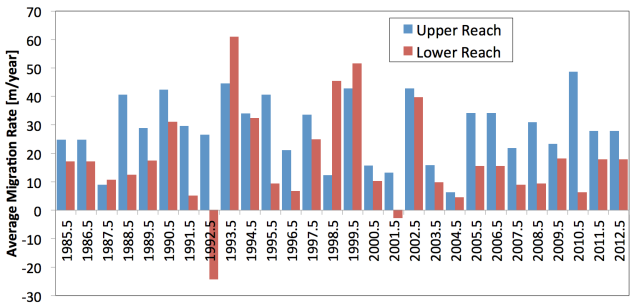

Figure 9: Migration Rates for Upper and Lower Reaches of the Jenaro-Herrera Bend

flow. M1 is on the upstream reach, M2 is near the town of Jenaro Herrera, and M3 is on the downstream reach. The higher velocities are located nearer to the outer bank, which are the banks on the upstream and downstream reach that are migrating closer together. In addition, there are secondary flow cells located near the outer bank where the velocity magnitude is greater.

3.4.2 Bed morphodynamics

Bathymetry measurements were obtained along the entire bend during May at a spacing of 500 meters at the upstream and downstream ends of the bend and at a spacing of 250 meters in the bend. Bathymetry measurements were taken at some locations during August as well, but only along portions of the bend. The measurements from May are represented as the bed of the river in Figure 10.

3.5 TWO-DIMENSIONAL RANS MODELING

3.5.1 The Model

The site will be modeled using a two-dimensional shallow water model with the turbulence closure model $k - \epsilon$. The software being used to model this is TELEMAC-2D, an open source CFD toolbox, because it uses parallel processing for computations it is useful for a large spatial scale, as described here (*EDF-DRD*, 2010). The numerical model solves a system of equations that includes one continuity equation and two momentum equations that are solved for the water depth and the velocity at each node, both in the streamwise and spanwise direction; three additional equations are solved for the turbulent kinetic energy, the dissipation of energy, and the turbulent viscosity; for details about the equations that are solved in this numerical model, and to see its application to a large river see *Frias et al.* (In Review). The boundary conditions are a constant discharge at the inlet, a constant elevation at the outlet, and non-slip boundary conditions at the banks.

3.5.2 The Methodology

The discharge input into the model is from acoustic Doppler current profiler (aDcp) measurements that were obtained on the Ucayali River during a measurement campaign in May 2013. The water surface elevation was obtained approximately 6.5 km upstream of the site at a gaging station maintained by the Peruvian National Service of Meteorology and Hydrology (SENAMHI). Since the next station downstream of Jenaro-Herrera is on the Amazon River, only the upstream gage was used to create the water surface, combined with a water surface slope of 0.0000274, calculated by Godoy for this portion of the Ucayali River. The boundaries of the water surface were obtained by digitizing a Landsat image from March 2013 (the only cloud-free image that was available near the date that measurements were taken). After the water surface was created, the process of creating the bed surface began. First, the original bathymetry points were sorted along the streamline, then the water depths of the points were subtracted from the water surface in order to get the bed elevation. After this was completed, an attempt was made to interpolate bed points using Matlab, but the results had some errors and, instead, Civil3D was used to create the bed surface manually. A structured mesh is used to model the geometry, with triangular elements that edge lengths of 50 m (Figure 10). The boundary conditions at the inlet and outlet for both the high discharge and low discharge cases are indicated in Figure 10.

The roughness will be calculated from the soil characterization of samples collected during an August field campaign.

3.5.3 Discussion

A main objective of modeling this bend is to determine what the shear stresses are along the banks. The model will be run and validated using the velocity profiles that were measured in May 2013.

3.5.4 The Results

Figure 13 compares the results of the model to the aDcp field measurements taken in May and August 2013. The patterns in the velocity at the three cross sections shown for each case reflect the measurements quite well, showing that the model gives a good representation of the reality, particularly in the sections of interest for studying a cutoff event. The numerical work for both low- and high-flows present high shear stresses near the outer banks, thus, I expect the meanders will be getting closer and produce a cutoff.

3.6 PREDICTION OF WHEN THIS BEND CUTOFF COULD OCCUR

Based on the analyses above, I am now better equipped to evaluate when a cutoff may occur. Using the temporal analysis of the satellite images, I have estimated that a cutoff could form in as little as 10 years if the cutoff occurs in the mechanism that I have described, if follows another mechanism, then the time scale for a cutoff may be more unpredictable. In addition, the Jenaro Herrera bend has a significant portion that is confined along one bank. This is different from the other two cases which I looked at, and may yield different results than I expect, perhaps making the time before a cutoff occurs even longer than expected.

3.7 DISCUSSION: WHAT ARE THE POSSIBLE IMPACTS?

This could have a major impact on the community, affecting the fishing industry and transportation in general. The town of Jenaro Herrera could become isolated from the Ucayali River and need new infrastructure, such as a road to access the river so that incoming goods can reach the town and so that farmers in Jenaro Herrera may get their products to market. Having a timescale for when the meander bend cutoff could occur can help in the planning process. In addition, a cutoff can affect the water levels upstream and downstream of the cutoff. On a positive note, a meander cutoff would shorten the route for people traveling

from other locations on the Ucayali River to the city of Iquitos, which has a market for selling produce, and oxbow lakes provide a unique habitat, important to the biodiversity in this region (*Guimaraes et al.*, 2000; *Penczak et al.*, 2003).

3.8 CONCLUSIONS

In this paper, I have used field measurements of bathymetry and velocity, data from gaging stations, satellite imagery, and a numerical model to study cutoff processes in the lower Ucayali River, a river that transitions from meandering to anabranching and is located in the Upper Amazon Basin. The review of previous cutoff events indicates that different cutoff mechanisms are possible on this portion of the river, showing that a prediction cannot be made with absolute certainty; however, there are two mechanisms that seem most probable. The first case is that the upper limb of the bend will collide with the lower limb. Measurements and modeling show that there are high shear stresses on the outer banks, which indicates that they should continue to erode, causing the two limbs of the bend collide. Assuming that the bend at Jenaro Herrera will continue to migrate at the current rate, a cutoff could occur in approximately 10 years from the end of the study period, around the year 2023. However, it is also possible that extreme floods in the coming years could cause a headcut channel on the downstream end of the bend to form a chute cutoff; if this happens, it is possible that one of the secondary channels, C2 or C3 in Figure 10, could become part of the main channel as in the downstream cutoff. Predicting the timeframe for this mechanism is much more difficult, as it relies heavily on hydrologic events over several seasons.

The isolation of a town due to a cutoff on a meander bend is a problem that can occur on meandering rivers throughout the Amazon basin. The purpose of this analysis was to study the mechanisms of cutoff in this river and to estimate a time scale for a cutoff to occur. The meander bend will continue to be monitored in the following years. If the estimate of the time scale is correct, this paper may provide a useful approach for assessing future cutoffs in the region, although these cutoffs depend on many factors.

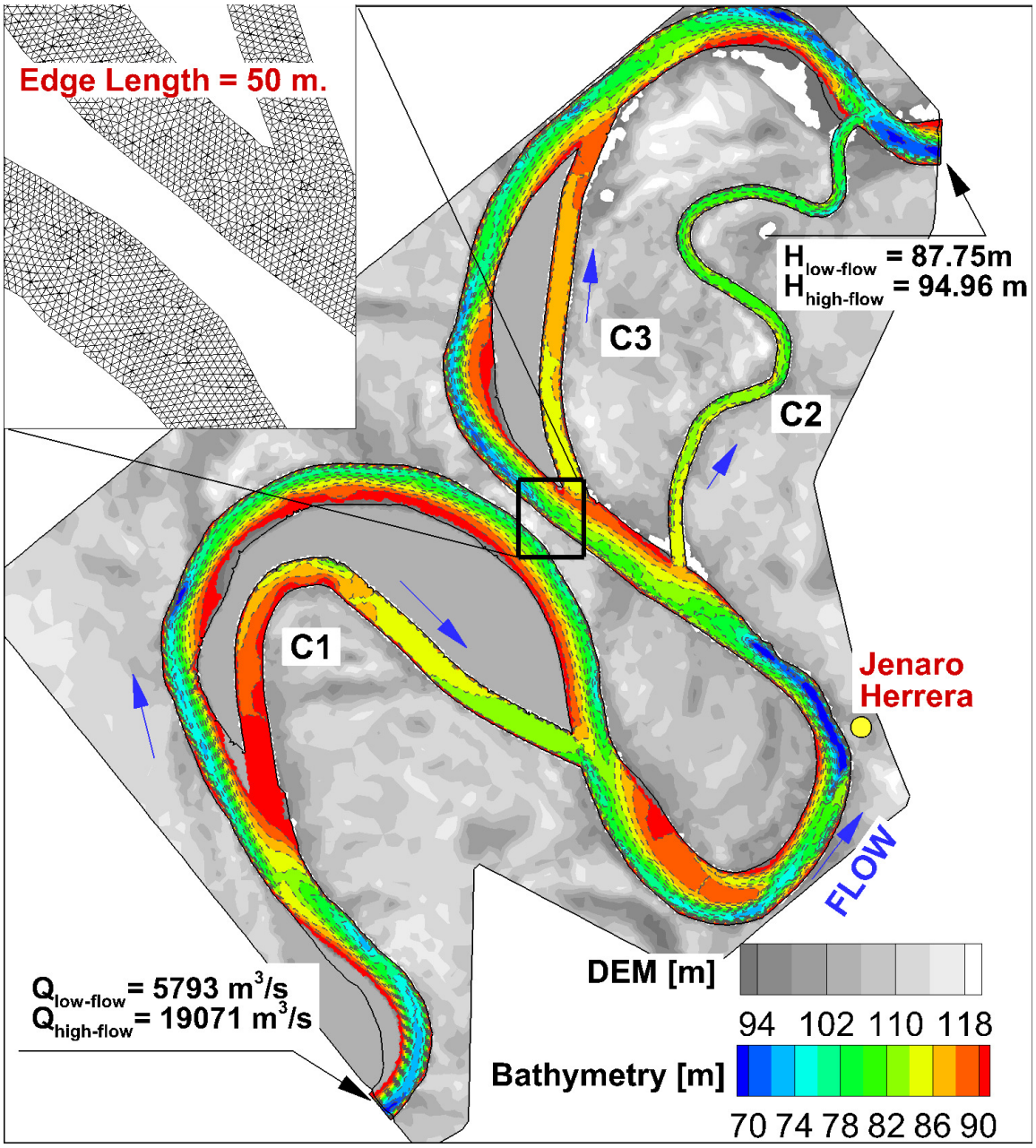

Figure 10: Mesh of Jenaro Herrera Bend.

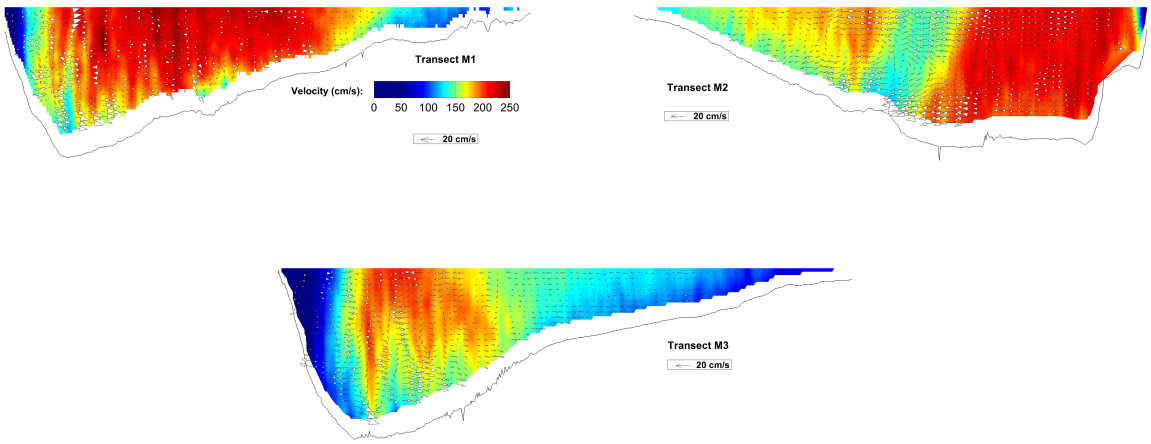

Figure 11: May velocity measurements. Velocity was measured at the locations shown in Figure 4C. M1 was measured on the upstream part of the bend, M2 was measured near the town of Jenaro Herrera, and M3 was measured on the downstream portion of the bend. The cross-sections show the downstream direction going into the page. The contours represent the velocity magnitude. The vectors represent the secondary flow using the Rozovskii decomposition. All of the cross-sections are shown at the same spatial scale.

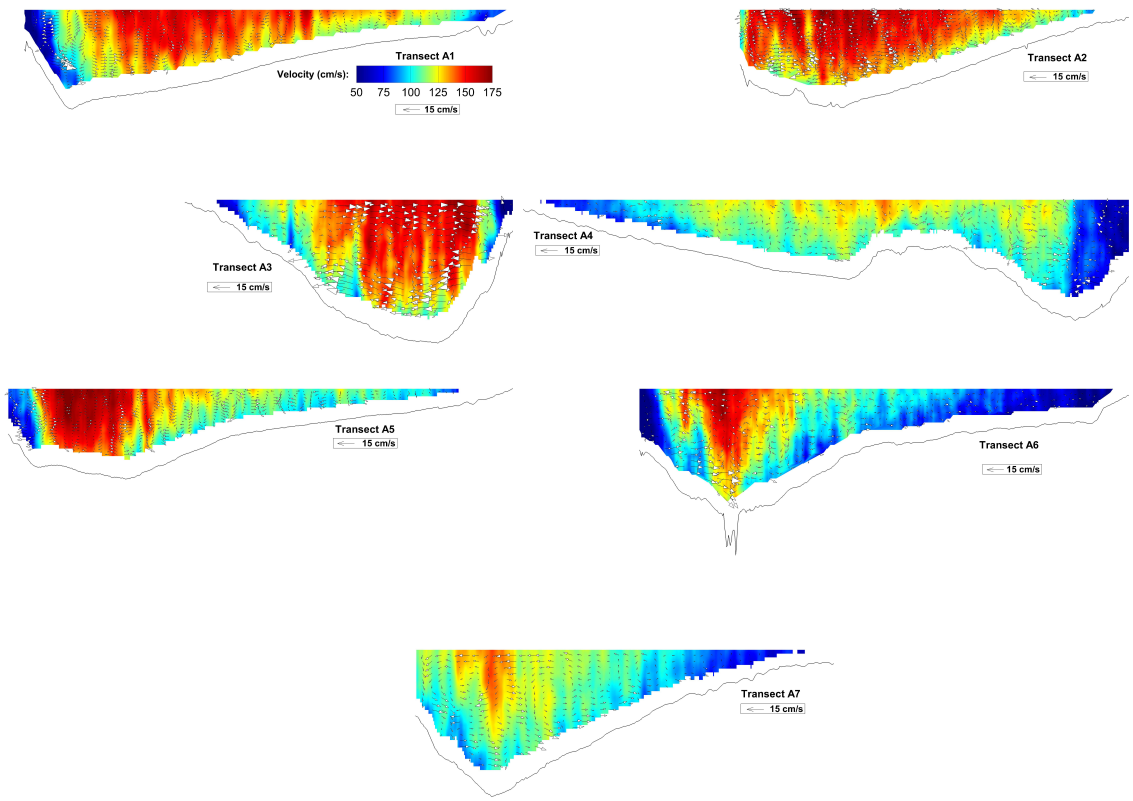

Figure 12: August velocity measurements. Velocity was measured at the locations shown in Figure 4C. The cross-sections are situated with the downstream direction going into the page. The contours represent the velocity magnitude. The vectors represent the secondary flow using the Rozovskii decomposition. Cross-sections are shown at the same spatial scale as the cross-sections in Figure 11.

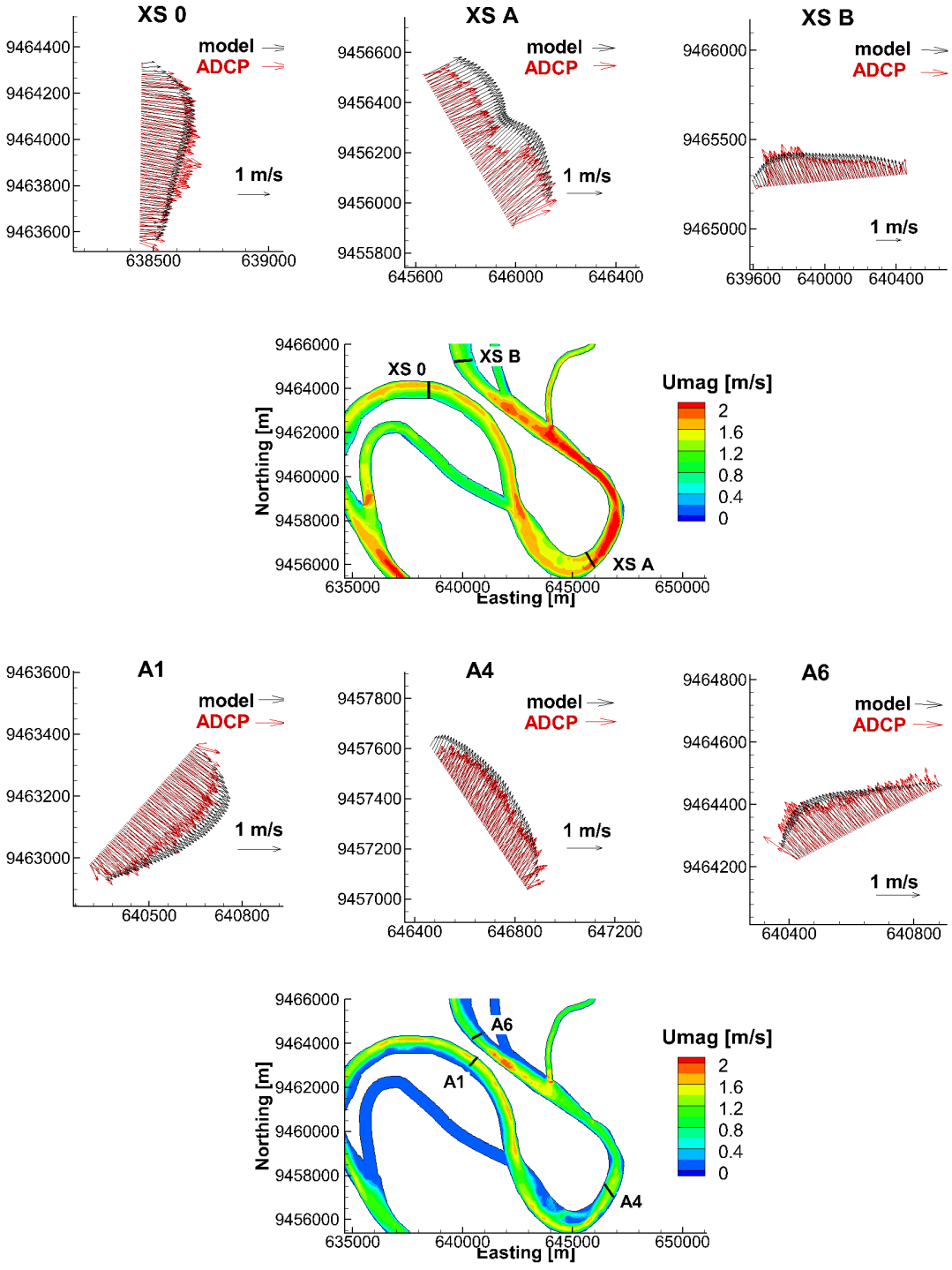

Figure 13: Modeling Results for Bend at Jenaro Herrera.

4.0 CONCLUSIONS

The Ucayali River is naturally dynamic and shows variation in characteristics, such as sinuosity, wavelength and number of channels, along its length. Knowledge of the existing characteristics and variations of the river, as well as understanding how the river moves over time are a necessary piece in understanding the complex relationship between climate and the river geomorphology. This work is not intended to give a comprehensive characterization of the whole river but, rather, to demonstrate methodologies for characterizing the river statically and dynamically.

Chapter 2 gives static characteristics of a reach of the Ucayali River, such as sinuosity and wavelength. This is the first step in developing a comprehensive method for static planform characterization of meandering rivers. Once the toolbox has had further testing, it will be available to the public.

Chapter 3 studies an important dynamic process on the Ucayali River, the meander bend cutoff. Satellite images were used to monitor evolution in the channel over time and to measure rates of channel migration. Field measurements were taken in the high and low season of 2013. These measurements are useful as inputs for the numerical model and for validation of the model. The velocity measurements and model show that there are high shear stresses on the outer bank of Jenaro Herrera, causing the banks to migrate closer together. In addition, these measurements can be used as a baseline to compare with future years.

5.0 FUTURE WORK

The meander statistics toolbox, mStat, in its current state calculates standard geometric characteristics of meandering streams, but the suite of tools could be increased to include an array of other variables, used in stream restoration design or in validation of numerical models, such as the variables described in *Howard and Hemberger* (1991); *Frascati and Lanzoni* (2009); *Camporeale et al.* (2005). To make the toolbox more accessible in the future, I would like to calibrate the toolbox to automatically select the correct level for the wavelet filter, based on the geometry of the river.

The meander bend at Jenaro Herrera continues to move as a result of the interaction between the hydrodynamics in the channel, seasonal flooding and the soil and vegetation. This area will continue to be monitored with field measurements annually in order to compare with the predictions and recalibrate, if necessary. A three-dimensional model of the bend may be run to better predict the mechanism and timescale of cutoff. In addition, I would like to collect sediment samples in the floodplain to improve our model.

BIBLIOGRAPHY

Abad, J. D., and M. H. Garcia (2009), Experiments in a high-amplitude kinoshita meandering channel. 1: Implications of bend orientation on mean and turbulent flow structure, *Water Resources Research*, *45*, doi:10.1029/2008WR007016.

Abizaid, C. (2005), An anthropogenic meander cutoff along the ucayali river, peruvian amazon, *Geographical Review*, *95*(1), 122–135.

Bodmer, R., F. Tula, P. Puertas, M. Antunez, and W. Bodmer (2011), Wildly fluctuating water levels in the amazon, *Biodiversity Science*.

Brice, J. (1974), Evolution of meander loops, *Geological Society of America Bulletin*, *85*(4), 581–586.

Camporeale, C., P. Perona, A. Porporato, and L. Ridolfi (2005), On the long-term behavior of meandering rivers, *Water resources research*, *41*(12).

Camporeale, C., E. Perucca, and L. Ridolfi (2008), Significance of cutoff in meandering river dynamics, *J. Geophys. Res. Earth Surface*, *113*(F1), doi:10.1029/2006JF000694.

Castello, L., D. G. McGrath, L. L. Hess, M. T. Coe, P. A. Lefebvre, P. Petry, M. N. Macedo, V. F. Renó, and C. C. Arantes (2013), The vulnerability of amazon freshwater ecosystems, *Conservation Letters*, *6*(4), 217–229.

Coomes, O., C. Abizaid, and M. Lapoint (2009), Human modification of a large meandering amazonian river: Genesis, ecological andeconomic consequences of the masisea cutoff on the central ucayali, peru, *Ambio*, *38*(3), 130–134.

D.E. Walling, B. W. (1996), *Erosion and Sediment Yield: Global and Regional Perspectives*, chap. Erosion and Sediment Yield: A Global Overview, pp. 3–19.

Dumont, J.-F. (1991), Fluvial shifting in the ucamara depression as related to the neotectonics of the andean foreland brazilian craton border (peru), *Géodynamique*, *6*(1), 9–20.

EDF-DRD (2010), *2D hydrodynamics TELEMAC-2D software Version 6.0 USER MANUAL*.

Espinoza, J., J. Ronchail, F. Frappart, W. Lavado, W. Santini, and J. Guyot (2013), The major floods in the amazonas river and tributaries (western amazon basin) during the 19702012 period: A focus on the 2012 flood*, *Journal of Hydrometeorology*, *14*, 1000–1008.

Espinoza, J. C., J. L. Guyot, J. Ronchail, G. Cochonneau, N. Filizola, P. Fraizy, D. Labat, E. de Oliveira, J. J. Ordoez, and P. Vauchel (2009a), Contrasting regional discharge evolutions in the amazon basin (19742004), *Journal of Hydrology*, *375*(34), 297 – 311, doi:http://dx.doi.org/10.1016/j.jhydrol.2009.03.004.

Espinoza, J. C., J. Ronchail, J. L. Guyot, G. Cochonneau, F. Naziano, W. Lavado, E. De Oliveira, R. Pombosa, and P. Vauchel (2009b), Spatio-temporal rainfall variability in the amazon basin countries (brazil, peru, bolivia, colombia, and ecuador), *International Journal of Climatology*, *29*(11), 1574–1594.

Ferguson, R. (1977), Meander sinuosity and direction variance, *Geological Society of America Bulletin*, *88*, 212–2–14.

Frascati, A., and S. Lanzoni (2009), Morphodynamic regime and longterm evolution of meandering rivers, *J. Geophys. Res. Earth Surface*, *114*(F2), doi:10.1029/2008JF001101.

Frias, C., A. Mendoza, J. Abad, J. Paredes, D. K., and H. Montoro (In Review), Morphodynamic stages of the anabranching in the upper amazon river basin, *Water Resources Research*.

Gagliano, S., and P. Howard (1984), The neck cutoff oxbow lake cycle along the lower mississippi river, in *River meandering*, edited by C. Elliot, pp. 147–158, ASCE.

Gay, G., H. Gay, W. Gay, H. Martinson, R. Meade, and J. Moody (1998), Evolution of cutoffs across meander necks in powder river, montana, usa, *Earth Surface Processes and Landforms*, *23*, 651–662.

Goulding, M., R. Barthem, and E. Ferreira (2003), *The Smithsonian Atlas of the Amazon*, Smithsonian Books, Washington, D.C.

Guimaraes, J. R. D., M. Meili, L. D. Hylander, M. Roulet, J. B. N. Mauro, R. A. de Lemos, et al. (2000), Mercury net methylation in five tropical flood plain regions of brazil: high in the root zone of floating macrophyte mats but low in surface sediments and flooded soils, *Science of the Total Environment*, *261*(1), 99–107.

Gutierrez, R. R., and J. D. Abad (2014), On the analysis of the medium term planform dynamics of meandering rivers, *Water Resources Research*.

Guyot, C. (2007), Impact socio-économique de la migration des méandres du fleuve ucayali sur la ville de pucallpa, Master's thesis, Université Aix-Marseille III.

Guyot, J., H. Bazan, P. Fraizy, J. Ordonez, E. Armijos, and A. Laraque (2007), Suspended sediment yields in the amazon basin of peru: A fi rst estimation, in *Water Quality and Sediment Behaviour of the Future*, pp. 3–10, Perugia, Italy.

Holeman, J. N. (2010), The sediment yield of major rivers of the world, *Water Resources Research*, *4*(4), 737–747.

Hooke, J. (1984), Changes in river meanders a review of techniques and results of analyses, *Progress in Physical Geography*, *8*(4), 473–508.

Howard, A. (1996), Modelling channel evolution and floodplain morphology, in *Floodplain Processes*, edited by M. Anderson, D. Walling, and P. Bates, pp. 15–62, Wiley.

Howard, A., and T. Knutson (1984), Sufficient conditions for river meandering: A simulation approach, *Water Resources Research*, *20*(11), 1659–1667.

Howard, A. D., and A. T. Hemberger (1991), Multivariate characterization of meandering, *Geomorphology*, *4*(3), 161–186.

Hudson, P., and R. Kesel (2000), Channel migration and meander-bend curvature in the lower mississippi river prior to major human modification, *Geology*, *28*(6), 531–534.

INICTEL - UNI, Dirección de Proyectos y Transferencia de Conocimientos (2009), Implementacin de una red de telecentros maynas y requena- distrito de saquena - iquitos : Actividades economicas.

Instituto Nacional de Estadistica e Informatica (2007), Censos nacionales 2007: Xi de población y vi de vivienda.

Lamotte, S. (1990), Fluvial dynamics and succession in the lower ucayali river basin, peruvian amazonia, *For. Ecol. Man.*, *33/34*, 141–156.

Lathrap, D. (1968), Aboriginal occupation and changes in river channel on the central ucayali, peru, *American Antiquity*, *33*(1), 62–79.

Latrubesse, E. M., J. Stevaux, and R. Sinha (2005), Tropical rivers, *Geomorphology*, *70*(3), 187–206.

Lauer, W. (2006), Nced stream restoration toolbox: Channel planform statistics.

Legleiter, C. J., and P. C. Kyriakidis (2006), Forward and inverse transformations between cartesian and channel-fitted coordinate systems for meandering rivers, *Mathematical Geology*, *38*(8), 927–958.

Lewis, G., and J. Lewin (1983), Alluvial cutoffs in wales and the borderlands, *Modern and ancient fluvial systems*, *6*, 145–154.

Miguez-Macho, G., and Y. Fan (2012), The role of groundwater in the amazon water cycle: 1. influence on seasonal streamflow, flooding and wetlands, *Journal of Geophysical Research: Atmospheres (1984–2012)*, *117*(D15).

Muller, F., F. Seyler, and J. Guyot (1999), Utilisation d'imagerie radar (ros) jers -1 pour l'obtention de réseaux de drainage. exemple du rio negro (amazonie), in *Hydrological and Geochemical Processes in Large Scale River Basins*, Manaus, Brazil.

Parsons, D., P. Jackson, J. Czuba, F. Engel, B. Rhoads, K. Oberg, J. Best, D. Mueller, K. Johnson, and J. Riley (2013), Velocity mapping toolbox (vmt): a processing and visualization suite for moving-vessel adcp measurements, *Earth Surf. Process. Landforms*, *38*, 1244–1260, doi:10.1002/esp.3367.

Parssinen, M., J. Salo, and M. E. Räsänen (1996), River floodplain relocations and the abandon- ment of aborigine settlements in the upper amazon basin: A historical case study of san miguel de cunibos at the middle ucayali river, *Geoarcheology*, *11*(4), 345–359.

Patel, P. L. (2013), Fluvial mechanics: Impact of climate change on sediment yield from river basins, *Hydrolink*, (3), 74–75.

Penczak, T., G. Zieba, H. Koszaliński, and A. Kruk (2003), The importance of oxbow lakes for fish recruitment in a river system, *Archiv für Hydrobiologie*, *158*(2), 267–281.

Pittman, L. R., and T. Salgado (1999), Carta geológica nacional:boletín 131 mapa geológico del cuadrángulo nauta.

Puhakka, M., R. Kalliola, M. Rajasilta, and J. Salo (1992), River types, site evolution and successional vegetation patterns in peruvian amazonia, *J. Biogeography*, *19*, 651–665.

Salonen, M., T. Toivonen, J. Cohalan, and O. Coomes (2011), Critical distances: Comparing measures of spatial accessibility in the riverine landscapes of peruvian amazonia, *Applied Geography*, *32*, 501–513.

Schumm, S., J. Dumont, and J. Holbrook (2000), *Active tectonics and alluvial rivers*, Cambridge University Press.

Seyler, F., F. Muller, G. Cochonneau, L. Guimaraes, and J. Guyot (2009), Watershed delineation for the amazon sub-basin system using gtopo30 dem and a drainage network extracted from jers sar images., *Hydrological Processes*, *23*(22), 3173 – 3185.

W.B. Langbein, S. S. (2013), Yield of sediment in relation to mean annual precipitation, *Transactions, AGU*, *39*(6), 74–75.

Wittmann, H., F. von Blanckenburg, L. Maurice, J. Guyot, N. Filizola, and P. W. Kubik (2011), Sediment production and delivery in the amazon river basin quantified by in situproduced cosmogenic nuclides and recent river loads, *GSA Bulletin*, *123*(5/6), 934–950.

Zinger, J., B. Rhoads, J. Best, and K. Johnson (2008), Flow structure and channel morphodynamics of meander bend chute cutoffs: A case study of the wabash river, usa, *J. Geophys. Res. Earth Surface*, *118*, 2468–2487, doi:10.1002/jgrf.20155.